Rarefied-Flow Aerodynamics Measurement Experiment on the Aeroassist Flight Experiment Vehicle

Robert C. Blanchard*
NASA Langley Research Center, Hampton, Virginia 23665

A flight experiment, called the Rarefied-Flow Aerodynamic Flight Experiment (RAME), is currently planned for the Aeroassist Flight Experiment (AFE) mission. This mission is a NASA sponsored precursor design tool for aeroassist orbital transfer vehicles. The RAME is one of 12 planned experiments on the AFE vehicle and will use flight measurements from accelerometers, rate gyros, and pressure transducers combined with knowledge of vehicle inflight mass properties and trajectory to achieve the primary objective of measuring aerodynamic forces and moments in the rarefied-flow environment, including transition into the hypersonic continuum. The experiment design utilizes preflight estimates of the aerodynamic measurements that are based on environment models, computer flowfield simulations, and ground test results. A secondary RAME objective is a postflight evaluation of the determination of vehicle mass properties from flight data. The experiment plan includes requirements for maneuvers that facilitate the determination of vehicle mass properties and aerodynamic characteristics. The aerodynamic maneuvers occur at several altitudes during flight. This provides an opportunity to examine gas-surface accommodation effects on aerodynamic coefficients in an environment of changing atmospheric composition. An overview is given on the RAME objectives, measurement domain, and anticipated results.

Nomenclature

a	= acceleration
a_m	= acceleration measurement vector
C	= aerodynamic force coefficient
$\bar{C}$	= normalized rarefied-flow aerodynamic coefficient factor, i.e., $(C-C_c)/(C_f-C_c)$
F	= jet thrust vector
F_{10}	= 10.7-cm solar flux
g	= gravitational acceleration at sea level
h	= altitude
I^{-1}	= inverse of the vehicle moment of inertia matrix
Kn	= Knudsen number, ratio of molecular mean free path to vehicle reference length
L/D	= lift-to-drag ratio
M	= mass
p,q,r	= angular rates about body axes, X_b, Y_b, and Z_b, respectively
R_a	= vector location of the accelerometer
R_j	= vector location of the jth control jet
S	= area
t	= time
V	= velocity
X_b, Y_b, Z_b	= body axes
α	= angle of attack
β	= angle of sideslip
ρ	= density
ω	= angular velocity vector

Subscripts

A	= axial
c	= continuum flow conditions
D	= drag
f	= free molecule flow conditions
L	= lift
m	= pitching moment
N	= normal
X	= component in X direction
Z	= component in Z direction
62	= 1962 U.S. standard atmosphere model

Presented as Paper 89-0636 at the AIAA 27th Aerospace Sciences Meeting, Reno, NV, Jan. 9–12, 1989; received May 24, 1990; revision received Dec. 27, 1990; second revision received Feb. 26, 1991; accepted for publication March 22, 1991.

*Aero-Space Technologist, Space Systems Division, Mail Stop 366. Senior Member AIAA.

Introduction

THE Aeroassist Flight Experiment (AFE) mission has been established by NASA to obtain aerodynamic, aerothermodynamic, and other flight data to aid the design of aeroassisted orbital transfer vehicles[1] (AOTVs). The Space Shuttle Orbiter will deploy the AFE vehicle into low Earth orbit where it will be accelerated back through the atmosphere to simulate a return of an AOTV. The AFE will carry 12 separate, but complementary, experiments designed to collect data on vehicle design technologies such as thermal protection systems, aerodynamics, radiative and convective heating rates data, and flight control.[2] The AFE trajectory is designed such that low-density, high-velocity flow phenomena can be readily investigated. These conditions cannot be fully duplicated in ground-based simulation facilities, thus providing the need for a flight experiment so that prediction techniques can be validated. The emerging tool for predicting vehicle rarefied-flow aerothermodynamic behavior is the direct simulation Monte Carlo (DSMC) technique.[3,4] As with any flowfield analyses method, validation and verification is required. Experiments on the AFE vehicle, including the Rarefied-Flow Aerodynamic Measurement Experiment (RAME), will provide these data. The primary objective of RAME is to measure in-flight aerodynamic force and moments in a rarefied-flow environment.

In addition to gathering flight data on vehicle performance, an opportunity exists after the flight to examine mass property determination capabilities. Information on spacecraft mass properties is generally obtained from preflight measurements and ground calculations based on predicted and measured consumables usage, configuration changes, and payload mass properties. Errors in these predictions can arise from incomplete modeling of operational consumption rates and imperfect

knowledge of payload properties. For a vehicle such as an AOTV, which must operate with a wide range of payloads, the likelihood of uncertainties in payload mass properties is high. However, control on vehicle mass property variations (e.g., c.g.) will be required in order to execute a shallow atmospheric pass. Of particular concern would be those payloads with poorly modeled or unknown mass properties, such as satellites of uncertain configuration or debris (e.g., expended boosters or natural artifacts such as asteroids).

All RAME objectives are to be achieved through flight measurements from various onboard instruments, including accelerometers, gyros, and pressure sensors, and ancillary measurements from a precision best estimated trajectory. This paper outlines the RAME objectives and goals, instrument and flight requirements (including maneuvers), data reduction, and anticipated results.

Aeroassist Flight Experiment Mission

Overview

The AFE vehicle will be used to investigate environmental and critical vehicle design technologies applicable to an AOTV. Here, Aeroassist refers to the technique by which a vehicle reduces its kinetic energy during an encounter with the atmosphere and then exits without making a complete entry.

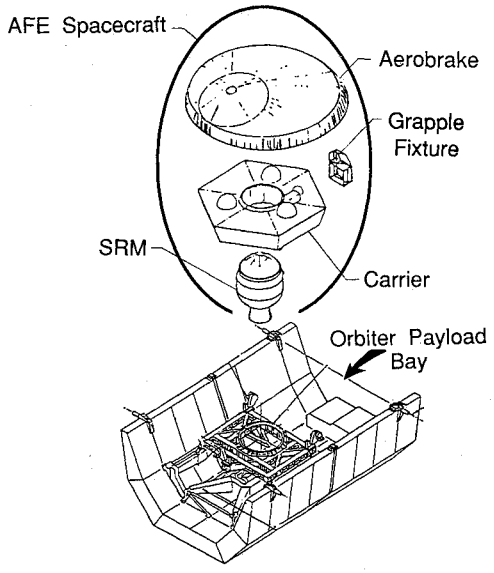

Fig. 1 AFE components and cradle in Orbiter payload bay.

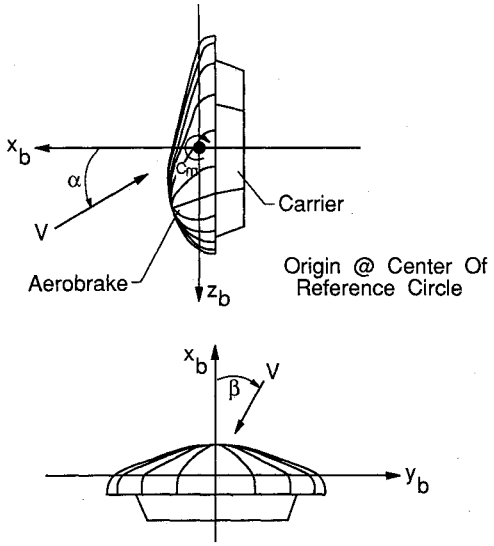

Fig. 2 Coordinate system definition.

Aeroassist technology can significantly enhance mission payload performance since payload can be substituted for braking fuel. The AOTV aerodynamic braking maneuvers only penetrate the upper regions of the atmosphere typically at or near geosynchronous orbit return velocities. Thus, the vehicle resides principally in the hypersonic rarefied flow regime throughout most of the mission.

Figure 1 is a schematic of the AFE spacecraft. The aerobrake, carrier vehicle, and solid rocket motor (SRM) are deployed from the Shuttle and comprise what is called the AFE spacecraft (or vehicle) in this report. The aerobrake is a raked off elliptical cone shape with a cone half angle of 60 deg and a rake angle of 73 deg, providing a blunt lifting body. Figure 2 shows this vehicle shape more clearly and defines the coordinate systems and sign conventions used in this report.

The AFE mission will carry the AFE spacecraft (Fig. 1) into orbit via the Shuttle Orbiter and deploy the spacecraft using the remote manipulator system (Fig. 3). After deployment, the AFE is propelled by a SRM into the Earth's atmosphere along a trajectory that simulates a spacecraft return from geosynchronous orbit. During the atmosphere pass, the AFE will be heavily instrumented in order to gather flight data on the AOTV technologies mentioned earlier. After an atmospheric pass (called aeropass phase), the spacecraft returns to orbit for retrieval by the Orbiter.

Aeropass Trajectory

The typical time history of the AFE spacecraft trajectory parameters, altitude and velocity, are given in Fig. 4a.[5] The velocity and altitude have been estimated using a trajectory program and the 1962 U.S. standard atmosphere.[6] About one orbit after deployment from the Shuttle in its circular orbit, a solid rocket ignites to lower the AFE vehicle periapsis during which velocity increases to about 33,000 ft/s, simulating a return from geosynchronous orbit. The velocity quickly decreases due to the atmosphere until, at about 170 s after the end of rocket motor burn, the velocity inflection point (corresponding to maximum acceleration) is reached. Thereafter, the velocity continues to drop more slowly (for about 2320 s) until orbit apogee is acquired. At this time, circularization and other maneuvers will be performed in order to rendezvous with the Orbiter. These are not shown in the figure. The principles of the aeroassist concept are clearly seen in Fig. 4a. Namely, a velocity increment δV of about 8200 ft/s is added to the spacecraft by a rocket motor. This δV is subsequently removed by the atmosphere during a round-trip excursion in altitude of about 740 kft and a time duration of about 2500 s.

Figure 4b shows additional trajectory information on angle of attack and the resulting effect on the normal-force and axial-force coefficients, C_N and C_A. Angle of attack is controlled by reaction jets at all altitudes, and plans include roll maneuvers to control the vehicle atmosphere penetration

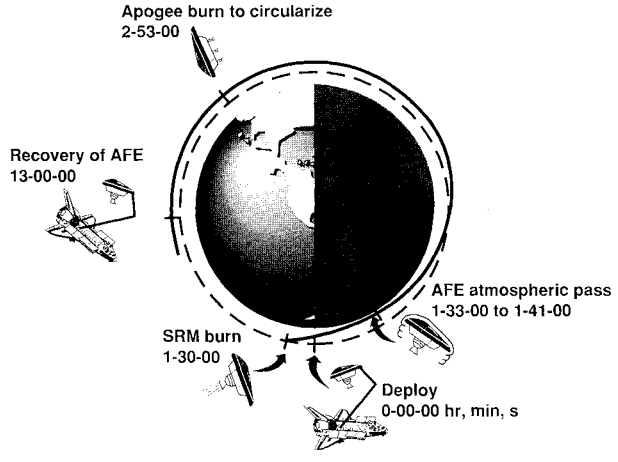

Fig. 3 AFE mission overview.

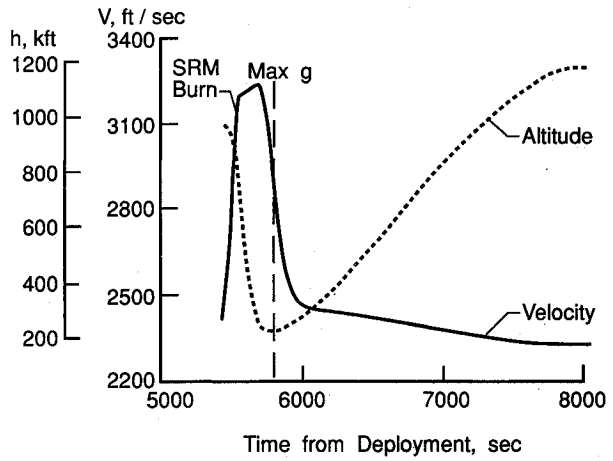

a) Velocity and altitude time profile

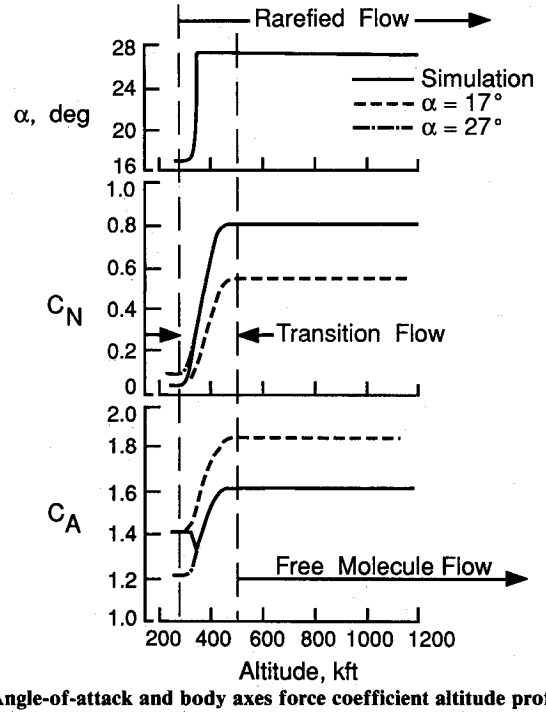

b) Angle-of-attack and body axes force coefficient altitude profiles

Fig. 4 Typical AFE trajectory.

depth. For the trajectory simulation shown, the attitude is held at 27 deg until about 330 kft, where it is modulated as shown in the figure to achieve the desired hypersonic trim angle of 17 deg. Correspondingly, the variations of the computed aerodynamic coefficients C_N and C_A are shown as solid curves in Fig. 4b.

Also shown in Fig. 4b are the coefficient limits for constant angles of attack of 17 deg and 27 deg. That is, at high altitudes (delineated by the right vertical line) are the free molecule flow coefficient values, whereas at low altitudes (delineated by the left vertical line) are the hypersonic continuum coefficient values. The transition region aerodynamic coefficients are based on the current AFE aerodynamic model, which includes an empirical bridging formula based upon Knudsen number, namely,

$$C = \sin^2[\pi(1/3 + 1/6 \log Kn)]$$

where $10^{-2} < Kn < 10$. Using a 1962 U.S. standard atmosphere model, the variation of each coefficient with altitude is calculated independent of the trajectory using

$$C_A = C_{Ac} + \bar{C}(C_{Af} - C_{Ac})$$

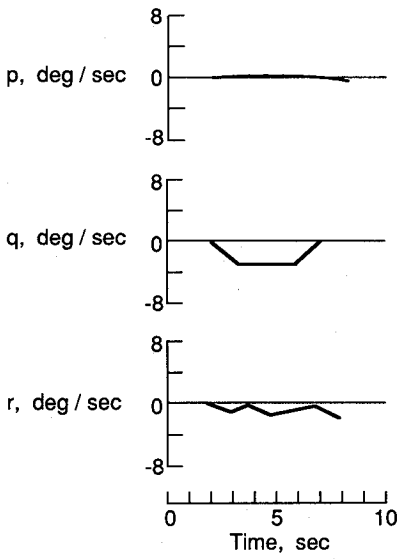

Fig. 5 Body axes rates associated with mass property simulation.

$$C_N = C_{Nc} + \bar{C}(C_{Nf} - C_{Nc})$$

These calculations are shown by dashed lines in the figure. It is seen that the largest change in both coefficients comes from transitioning from free-molecule flow to continuum flow. During this time, C_N changes dramatically due to shear effect (almost an order of magnitude), whereas C_A changes about 25% mostly due to pressure effects. The C_N and C_A variations shown will affect acceleration measurements aligned with the body axes discussed later.

Experiment Objectives and Goals

Rarefied-Flow Aerodynamics

The primary objective of the RAME is to provide flight measurements of the AFE vehicle aerodynamic performance characteristics (C_N, C_A, and C_m) in the rarefied-flow regime, i.e., through the transition from continuum flow into the free-molecule flow. For the prediction of aerodynamic forces under transitional flow conditions, it is necessary to rely on approximate theories[7,8] and a relatively small collection of experimental data; some collected in ground facilities[9] and some from flight experiments.[10,11] Thus, the flight results from the RAME on the AFE vehicle will provide a significant increase in the flight data base.

Mass Property Determination

The secondary objectives of RAME include a technology demonstration of in-flight mass property determination (e.g., vehicle moment of inertia, mass, and c.g. locations). On-orbit flight control systems are often made robust relative to mass properties, i.e., capable of tolerating a fixed wide range of mass properties, beyond which the systems are unstable. Even within that range, performance depends on accurate knowledge of mass properties.

Stability and control of a vehicle in atmospheric flight strongly depend on the separation distance between the vehicle center of gravity and the aerodynamic center. Accurate determination of the center of gravity is thus necessary for safety of flight. Accurate in-flight measurement of the center of gravity would enhance confidence in flight safety for a vehicle with a widely varying configuration, with large propellant mass fraction, and with a wide range of payloads.

The general approach to mass property determination is based on a technology developed for potential space station adaptive control application.[12] For AFE application, the technique is more fully discussed in Ref. 13. In summary, when a

control force, such as a jet firing, is applied to a spacecraft, the accelerometer response is

$$a_m = F/M + \omega \times R_a + \omega \times \omega \times R_a$$

A rate gyro on the spacecraft would detect a rate change

$$\delta\omega = I^{-1}(R_j \times F)\,\delta t$$

where δt is the rate gyro sampling interval.

Clearly, these equations cannot be solved explicitly for R_a, M, and I^{-1}. To resolve this, a nonlinear filter, similar to the extended Kalman filter, compares accelerometer and rate gyro measurements with predictions of those measurements in response to jet firings and derived estimates of R_a, M, and I^{-1}. In addition, the filter uses redundant measurements to minimize the impact of sensor noise on the accuracy of its estimates. Required inputs are control placement, direction and magnitude of control forces, and torques. No prior estimates of mass properties or environment disturbances are necessary.

A maneuver sequence of jet firings will be selected before flight to maximize the improvement in the mass property estimates. Figure 5 shows an example of resulting angular rates for a series of 12 jet firings over a period of approximately 12 s. Rate gyros used for navigation will provide the measurement of these rates (combined with the RAME accelerometers output) to be used in the process performed postflight.

Preliminary studies indicate that mass property determination can be performed with accuracy as shown in Table 1. Initial values of the estimates are numerically zero, corresponding to no initial guess. These results include digitization effects of the rate gyros and accelerometer but assume perfect instrument alignment and perfect jet firings. As a result, these are optimistic calculations.

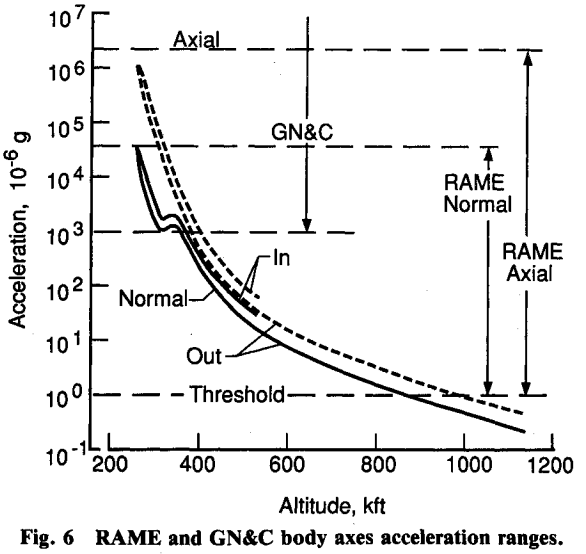

Fig. 6 RAME and GN&C body axes acceleration ranges.

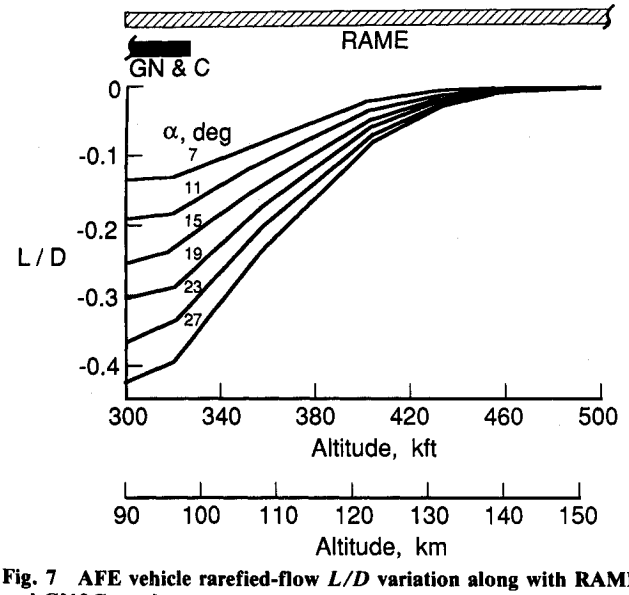

Fig. 7 AFE vehicle rarefied-flow L/D variation along with RAME and GN&C accelerometer coverage.

Experiment Measurement Ranges

Accelerometer Ranges

The RAME accelerometer hardware design is derived from the High Resolution Accelerometer Package (HiRAP) Shuttle Orbiter Experiment Program, which to date has successfully flown on 10 Shuttle Orbiter missions.[14] Shuttle Orbiter rarefied-flow aerodynamic performance data, principally L/D, have been obtained on each flight as well as density variations in the upper middle atmosphere (i.e., from 200 to 330 kft).[15] Improvement in empirical prediction of transitional behavior has been made with the flight data for the winged reentry class of vehicles. However, vehicle shape dependence continues to be an open issue.

A dedicated linear accelerometer package will be utilized for the RAME flight acceleration measurements, since the RAME measurement regime is beyond the capabilities of the baseline guidance, navigation, and control (GN&C) system. Figure 6 shows the approximate relationship between the expected normal and axial axis thresholds of the GN&C and the RAME in terms of altitude coverage. These have been calculated from

$$a_i = \tfrac{1}{2}\rho_{62} V^2 C_i (S/M)$$

where $i = A$ or N, and the velocity V and the coefficients C_i are from the aforementioned simulation.

Figure 7 shows the altitude ranges over which acceleration ratios can be obtained from each set of sensors (top of figure). Also shown is the expected L/D variation in the rarefied-flow transition regime as a function of angle of attack. This figure shows approximately where the GN&C instrument capabilities end in terms of the performance parameter, L/D, and altitude.

Atmospheric Variations

Figure 8 shows the anticipated variation of the axial acceleration component with the solar cycle, indicated by the 10.7-cm solar flux index F_{10}, (60 and 250 correspond to solar minimum and solar maximum, respectively). The calculations use a density model that is a combination of a middle atmosphere reference model by Barnett and Corney[16] and the MSIS-83 model.[17] The MSIS-83 model is a complete global model in the sense that all known variables that have a significant influence in atmosphere density are incorporated, such as solar flux,

Table 1 Preliminary results of Aeroassist Flight Experiment mass property determination simulation

Parameter	True value	Estimate	Absolute error
Inverse inertia matrix $\times 10^{-3}$ (slug-ft^2)$^{-1}$			
I^{-1} (1, 1)	0.6402	0.6400	−0.0001
I^{-1} (1, 2)	0.0	0.00001	0.00001
I^{-1} (1, 3)	−0.000007	−0.0000003	0.0000074
I^{-1} (2, 2)	0.6436	0.6436	−0.000016
I^{-1} (2, 3)	0.0	0.0000081	0.0000081
I^{-1} (3, 3)	0.6480	0.6480	0.000018
Center-of-gravity location, ft			
X	5.9580812	5.9580850	−0.0000038
Y	0.0	−0.000081	0.0000816
Z	−0.0001122	−0.000031	−0.0001090
Mass reciprocal, slug^{-1}			
M^{-1}	0.004249	0.004250	−0.0000009

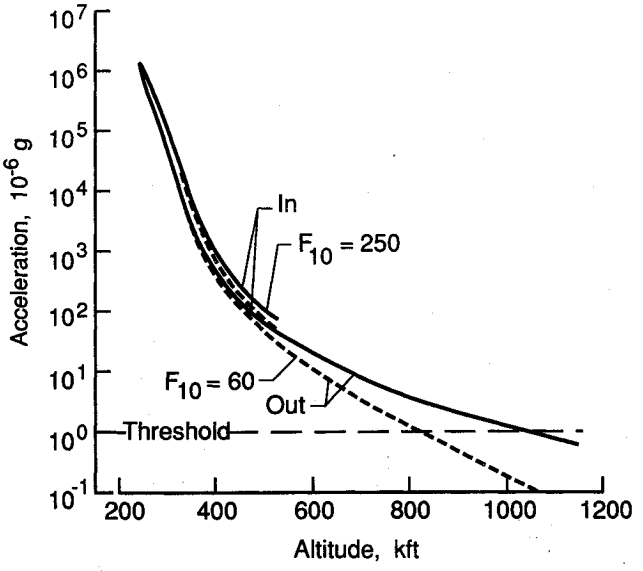

Fig. 8 Axial acceleration variation with solar cycle.

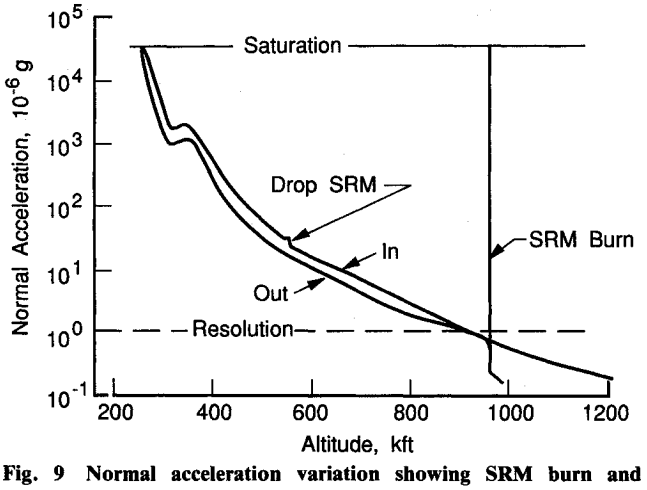

Fig. 9 Normal acceleration variation showing SRM burn and release.

geomagnetic activity, and annual/semiannual effects. For the variations shown in Fig. 8, the extremes in solar flux index were used with a low geomagnetic index along the AFE ground track. As expected, the largest influence in measurements would occur at higher altitudes. A change of about 575 kft in coverage is expected at instrument threshold. There are negligible effects below about 330 kft. Not shown are the corresponding results of the normal component, which show essentially the same variation.

Mass Variations

The previous graphs, Figs. 6 and 8, show acceleration-altitude profiles that do not include the segment of the trajectory that encompasses the rocket motor burn. For completeness, Fig. 9 shows the typical variation of the normal acceleration that is expected to occur with the rocket burn and the subsequent dropping of the spent rocket motor casing. As seen, upon rocket ignition at about 984 kft, the channel saturates, and upon returning on scale, it shifts to a larger acceleration due to a mass change. Approximately 45 s later, the rocket motor casing is separated and another jump in acceleration level occurs. (The separation event itself is not shown.) The axial acceleration basically contains the same features but is not shown.

Pressure Transducer Range

A pressure transducer with a maximum range of 0.01 psia will be used in the RAME to provide an independent measurement of the local atmosphere conditions during flight. This transducer is connected to an orifice located near the AFE vehicle stagnation point. Figure 10 shows the approximate altitude region covered by the RAME pressure measurements. The curve labeled p_{stag} is the predicted stagnation pressure of the AFE vehicle in rarefied flow. The curve is a combination of computational data from a three-dimensional viscous code, which includes chemical and nonequilibrium flow,[18] in conjunction with data from a three-dimensional Monte Carlo simulation.[19] Figure 10 also shows a curve of chamber pressure, labeled $p_{chamber}$, which is the pressure registered by the pressure transducer under the assumption that the gas is fully thermally equilibrated. This curve is an estimate based on earlier work done for the Shuttle Orbiter nose region, which includes an orifice at angle of attack on a hyperboloid.[20,21]

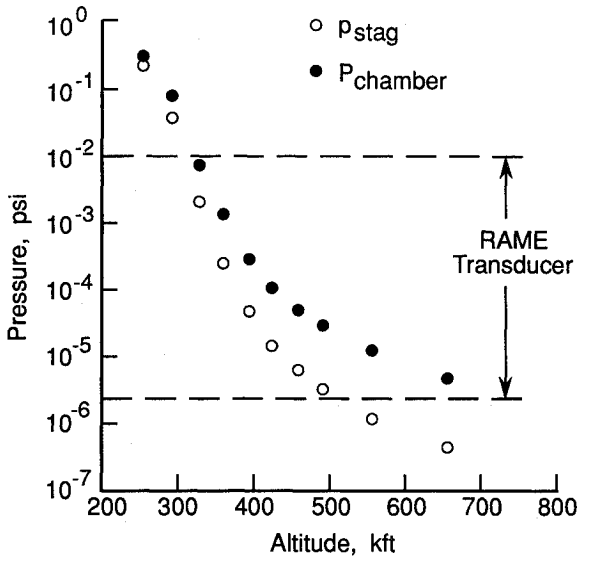

Fig. 10 Approximate RAME stagnation pressure transducer range.

The voltage output of the transducer is connected to a 12-bit analog-to-digital converter. This provides a means to estimate the lowest pressure reading, i.e., the resolution, which is also shown in Fig. 10. Thus, the extent of coverage is to about 500 kft, which includes most of the rarefied-flow transition flight regime. At higher altitudes, pressure estimates based on an atmosphere model that match the flight pressure measurements as a boundary condition will be used. For the region below about 325 kft, the RAME instrument saturation location, pressure transducers from other experiments will operate over the rest of the hypersonic flow regime.

Other Instruments

The implementation of an aerodynamic flight experiment requires additional instrumentation, principally gyros. The gyro system provides fundamental measurements used to determine aerodynamic moments, attitude information, and induced linear accelerations due to rotation about the center of gravity. The AFE GN&C gyros provide changes in vehicle attitude from which angular body rates are derived. This system uses ring-laser gyros, which resolve changes in angles to about 8.74×10^{-4} deg and have very stable scale factors. In addition, data from postflight characterization of the trajectory parameters (e.g., vehicle velocity) are also required. The generation of trajectory parameters data depends on several instruments, such as tracking data in conjunction with data from the GN&C package. Data to identify thruster control activity will also be available from flight along with the measured and monitored mass properties of the AFE vehicle.

Experimental Flight Profile

A typical RAME flight operation profile is shown in Fig. 11 in conjunction with the AFE mission major event time line for

the aeropass mission phase and corresponding acceleration profiles. The bottom figure shows the expected level of acceleration in the axial and normal channel due to the aerodynamic loads. Included, for perspective, are the expected levels of acceleration spikes due to control jet thruster firings. The middle of the figure shows some of the mission events that will occur during this phase of the mission. Two events of particular significance are the separation of the SRM casing (annotated as Drop SRM) and the location of the inbound and outbound entry interface (arbitrarily defined as 400 kft). During the AFE mission, periods of time are allocated for gathering data for determination of postflight mass properties and rarefied flow aerodynamic coefficients as a function of α and β, labeled Aerodynamic Maneuvers. These are discussed separately in the following paragraph. Specific mass property maneuvers will also be performed beyond the effects of the sensible aerodynamics, both before and after the aeropass phase, in order to provide data for postflight mass properties determination. These maneuvers consist of providing torques about each of the three axes and, in addition, a no-couple jet firing, which results in a small translation. During these maneuvers, the GN&C and RAME instruments will be operating and, in addition, jet firing histories will be recorded.

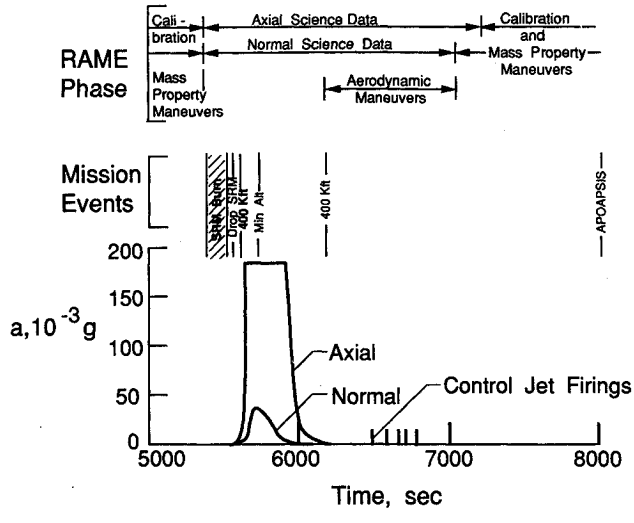

Fig. 11 RAME flight operation profile during AFE aeropass mission phase.

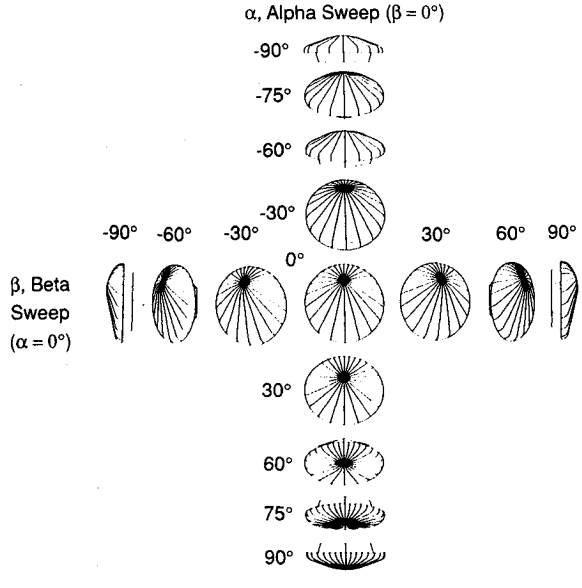

Fig. 12 Views of AFE vehicle during RAME aerodynamic maneuver sequence (velocity vector directed toward viewer).

As the vehicle exits the atmosphere, rarefied-flow aerodynamic coefficient data are obtained as a function of α and β. These data periods are labeled Aerodynamic Maneuvers in Fig. 11. At three altitudes (350, 500, and 650 kft) during the outward trajectory, a maneuver sequence is performed that includes independent sweeps of both α and β from -90 to $+90$ deg. A fourth maneuver sequence will be executed at orbital altitudes for calibration purposes. A snapshot representation of the α-β sweep maneuvers for 30-deg increments is presented in Fig. 12. Each maneuver occurs at the rate of 5 deg/s. The principal reason for obtaining samples at different altitudes is to obtain information on a major unknown in the prediction of rarefied-flow aerodynamics, namely the surface reflection/accommodation effects. Currently, a priori prediction of the rarefied-flow aerodynamics is limited because of the lack of information on gas-surface molecular interactions. The AFE offers an unprecedented opportunity to gather flight information to support surface accommodation theory development. The outbound trajectory inherently provides two major benefits to the problem: 1) the heat pulse from the atmosphere friction acts as a surface cleansing agent, and 2) the vehicle surface will be subjected to bombardment predominantly from molecular nitrogen N_2, at low altitudes and then, at higher altitudes, predominantly from highly reactive atomic oxygen O. Thus, progressive changes in the aerodynamic coefficients with altitude, other than rarefaction effects, should contribute to an understanding of the behavior of surface accommodation. Figure 13 illustrates the approximate change in atmospheric composition for the major species as a function of altitude using the 1976 U.S. standard atmosphere model.[22] Inserted are the locations of the planned maneuvers with the approximate altitude change (i.e., α-β maneuver window) for each maneuver sequence.

Anticipated Results

The data from RAME will provide the aerodynamic force coefficients C_N and C_A (or C_L and C_D), the force ratio N/A (or L/D), and the aerodynamic moments (e.g., C_m) in the rarefied-flow regime using techniques developed under previous Shuttle Orbiter flight experiments.[23] Estimates of the predictions of the aerodynamics of the AFE vehicle are shown in Figs. 14a and 14b. Figure 14a is a compilation of several sources of data that predict the AFE vehicle rarefied flow, in-

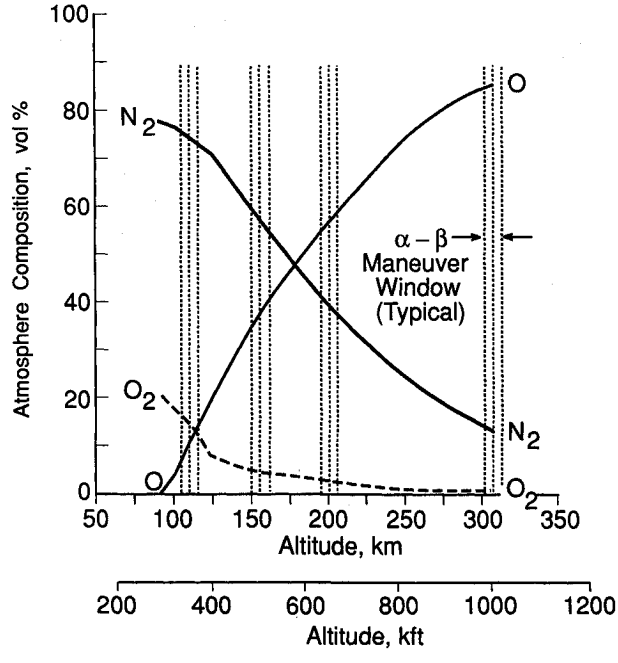

Fig. 13 Atmosphere composition during RAME aerodynamic maneuvers (1976 U.S. standard atmosphere).

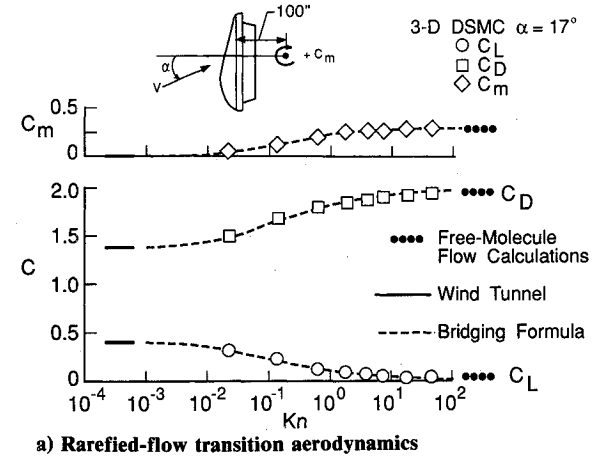

a) Rarefied-flow transition aerodynamics

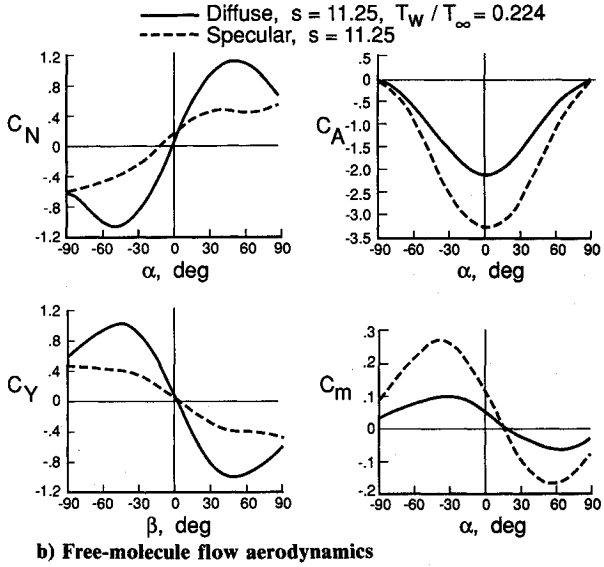

b) Free-molecule flow aerodynamics

Fig. 14 AFE vehicle force and moment predictions.

cluding transition aerodynamics as a function of Knudsen number (reference length = 14 ft). The hypersonic continuum values are mostly from tunnel data,[24] and the free-molecule values shown are derived from calculations,[25] (complete diffuse surface reflection is shown). The moment reference center for this figure is placed 100 in. aft of the center of the reference center in agreement with the AFE project data base. The transition data between the flow extremes are from Monte Carlo calculations mentioned earlier.[19] A new empirical bridging formula is used and is given as

$$C = \sin^n[\pi(3 + \log Kn)/10]$$

where

$$10^{-3} < Kn < 100$$

$$n = (7 - \log Kn)/5$$

Figure 14b shows the predictions of AFE vehicle aerodynamics for the α-β sweeps in the free-molecule regime. These calculations, reproduced from Ref. 24, show the effect of two surface reflection assumptions for all of the force components and the pitching moment coefficient.

Figure 15 shows, as an example, the type of results expected with RAME. Shown are the flight results of a Viking I entry vehicle (a 70-deg half-cone angle), which has a shape similar to the AFE vehicle. Included on the figure are three-dimensional DSMC calculations for the AFE at −17 deg. There is

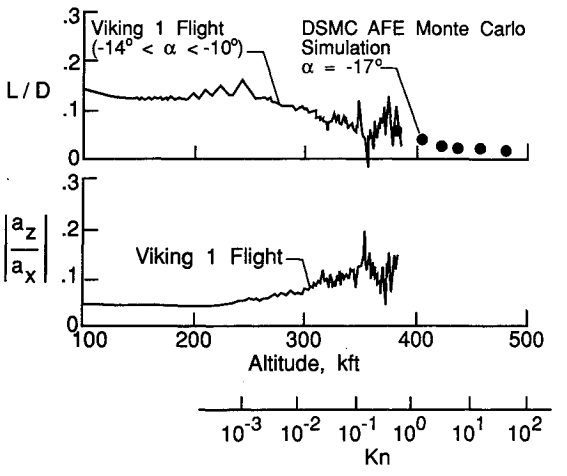

Fig. 15 Comparison of Viking I flight *L/D* with AFE simulation.

reasonably good agreement with the general trend of the flight data. The Viking trim attitude was near −11 deg and experienced about ±2 deg attitude excursions when switched from attitude hold control to rate damping control at about 260 kft. The principal objective for RAME is to provide the measurement capability to cover the entire rarefied regime. This was not a consideration during the Viking mission.

Summary

An experiment is being developed to provide measurements on aerodynamics of a blunt lifting-body vehicle in the hypersonic rarefied-flow flight regime, including transition into the continuum. The experiment, called the Rarefied-Flow Aerodynamics Measurement Experiment, is one of a complement of 12 interrelated investigations that comprise the Aeroassist Flight Experiment mission. The data obtained from this experiment will address key aeroassisted orbital transfer vehicle design and technology issues in the areas of aerodynamics and control and in computational fluid dynamic code verification using flight data. This should significantly enhance the current data base since the data from the experiment cannot be obtained in current ground facilities. A secondary objective of the experiment is to provide an in-flight mass property technology determination (e.g., vehicle mass, center-of-gravity location, and moments of inertia). This postflight demonstration should provide the data for robust control theory formulations, which are applicable to special AOTV payloads, such as return of unspecified satellites, debris, and asteroids. The RAME includes a triaxial accelerometer package with a resolution of $1/10^{-6}$ g, a 0.01-psia stagnation pressure transducer, and a rate gyro system that is part of the vehicle GN&C package. Other elements of the experiment (e.g., mass, thruster events, etc.) come from various AFE engineering subsystems. The design of the experiment includes aerodynamic and mass property maneuvers. The aerodynamic maneuvers will be performed over a range of angles of attack and sideslip at several altitudes (about 350, 500, and 650 kft) in the rarefied-flow regime. These maneuvers allow measurements of the vehicle aerodynamics under a variety of flow conditions and thereby provide information on the effects of surface accommodation on aerodynamic coefficients. Sensor range requirements are based on studies of the predicted behavior of the vehicle in the rarefied-flow environment. After the flight, comparisons will be made between the experimental flight data and predicted data bases.

Acknowledgments

The author wishes to recognize E. V. Bergmann (Charles Stark Draper Laboratory) for his significant contributions to the computations and formulation of the mass property aspects of this experiment, and E. W. Hinson (ST Systems

Corporation), J. Y. Nicholson (Vigyan Research Associates), and J. Ritter (Lockheed Engineering & Sciences Corporation) for their computational contributions and assistance in the development of the concepts of this experiment.

References

[1]Walberg, G. D., "A Survey of Aeroassisted Orbit Transfer," *Journal of Spacecraft and Rockets,* Vol. 22, No. 1, 1985, pp. 3–18.

[2]Jones, J. J., "The Rationale for an Aeroassist Flight Experiment," AIAA Paper 87-1508, June 1987.

[3]Bird, G. A., "Low Density Aerothermodynamics," AIAA Paper 85-0994, June 1985.

[4]Dogra, V. K., Moss, J. N., and Simmonds, A. L., "Direct Simulation of Aerothermal Loads for an Aeroassist Flight Experiment Vehicle," AIAA Paper 87-1546, June 1987.

[5]French, R. A., private communication, Sept. 1988.

[6]Anon., *U.S. Standard Atmosphere, 1962,* NASA, USAF, USWB, Dec. 1962.

[7]Hurbut, F. C., and Sherman, F. S., "Application of the Nocilla Wall Reflection Model to Free-Molecule Kinetic Theory," *Physics of Fluids,* Vol. 11, March 1978, pp. 486–496.

[8]Potter, J. L., "Transitional, Hypervelocity Aerodynamic Simulation and Sealing," *Thermophysical Aspects of Re-entry Flows,* Vol. 103, *Progress in Astronatics and Aeronautics,* edited by J. N. Moss and C. D. Scott, AIAA, New York, 1986, pp. 79–96.

[9]Koppenwallner, G., "The Drag of Simple Shaped Bodies in the Rarefied Hypersonic Flow Regime," AIAA Paper 85-0998, June 1985.

[10]Blanchard, R. C., and Walberg, G. D., "Determination of the Hypersonic-Continuum/Rarefied-Flow Drag Coefficient of the Viking Lander Capsule I Aeroshell from Flight Data," NASA TP-1793, Dec. 1980.

[11]Blanchard, R. C., and Buck, G. M., "Rarefied-Flow Aerodynamics and Thermosphere Structure from Shuttle Flight Measurements," *Journal of Spacecraft and Rockets,* Vol. 23, No. 1, 1986, pp. 18–24.

[12]Bergmann, E. V., Walker, B. K., and Levy, D. R., "Mass Property Estimation for Control of Asymmetrical Satellites," *Journal of Guidance, Control, and Dynamics,* Vol. 10, No. 5, 1987, pp. 483–491.

[13]Bergmann, E. V., and Blanchard, R. C., "In-Flight Demonstration of Mass Property Identification on the Aeroassist Flight Experiment," Society of Allied Weight Engineers, Paper 1887, May 1989.

[14]Blanchard, R. C., and Rutherford, J. F., "Shuttle Orbiter High Resolution Accelerometer Package Experiment: Preliminary Flight Results," *Journal of Spacecraft and Rockets,* Vol. 22, No. 4, 1985, p. 474.

[15]Blanchard, R. C., Hinson, E. W., and Nicholson, J. Y., "Shuttle High Resolution Acceleration Package Experiment Results: Atmospheric Density Measurements Between 60–160 Km," *Journal of Spacecraft and Rockets,* Vol. 26, No. 3, 1989, pp. 173–180.

[16]Barnett, J. J., and Corney, M., "Middle Atmosphere Reference Model Derived from Satellite Data," *Middle Atmosphere Program (Handbook for MAP),* Vol. 16, edited by K. Labitzke, J. J. Barnett, and B. Edwards, July 1985, pp. 47–85.

[17]Hedin, A. E., "A Revised Thermospheric Model Based on Mass Spectrometer and Incoherent Scatter Data: MSIS-83," *Journal of Geophysical Research,* Vol. 88, Dec. 1983, pp. 10170–10188.

[18]Gnoffo, P. A., private communication, NASA Langley Research Center, Hampton, VA, July 1990.

[19]Celenligil, M. C., Moss, J. N., and Blanchard, R. C., "Three-Dimensional Flow Simulation About the AFE Vehicles in the Transitional Regime," AIAA Paper 89-0245, Jan. 1989.

[20]Bienkowski, G. K., "Inference of Free Stream Properties from Shuttle Upper Atmosphere Mass Spectrometer (SUMS) Experiment," *Rarefied Gas Dynamics,* Vol. 1, edited by H. Oguchi, University of Tokyo Press, Tokyo, Japan, 1984, pp. 295–302.

[21]Moss, J. N., and Bird, G. A., "Monte Carlo Simulations in Support of the Shuttle Upper Atmospheric Mass Spectrometer Experiment," AIAA Paper 85-0968, June 1985.

[22]Anon., *U.S. Standard Atmosphere, 1976,* NOAA, NASA, USAF, Oct. 1976.

[23]Blanchard, R. C., Hendrix, M. K., Fox, J. C., Thomas, D. J., and Nicholson, J. Y., "The Orbital Acceleration Research Experiment," *Journal of Spacecraft and Rockets,* Vol. 24, No. 6, 1987, pp. 504–511.

[24]Wells, W. L., "Measured and Predicted Aerodynamic Coefficients and Shock Shapes for the Aeroassist Flight Experiment (AFE) Configuration," NASA TP-2956, Jan. 1990.

[25]Blanchard, R. C., and Hinson, E. W., "Free-Molecule-Flow Force and Moment Coefficients of the Aeroassist Flight Experiment Vehicle," NASA TM -101600, July 1989.

James E. Daywitt
Associate Editor